

Gas transport properties of polysulphones: 1. Role of symmetry of methyl group placement on bisphenol rings

J. S. McHattie, W. J. Koros and D. R. Paul*

Department of Chemical Engineering and Center for Polymer Research,
The University of Texas at Austin, Austin, Texas 78712, USA

(Received 6 February 1990; accepted 23 March 1990)

Gas sorption and transport properties are reported for a series of polysulphones having either two or four phenylene hydrogens per repeat unit replaced with methyl groups. The results for tetramethyl bisphenol A polysulphone (TMPSF), dimethyl bisphenol A polysulphone (DMPSF) and dimethyl bisphenol Z polysulphone (DMPSF-Z) are compared to unsubstituted bisphenol A polysulphone (PSF). The effect of the substituents on chain mobility and chain packing has been related to the gas transport properties. Dynamic mechanical thermal analysis and differential scanning calorimetry were used to judge chain mobility, while X-ray diffraction and free-volume calculations give information about chain packing. Permeability measurements were made for He, H₂, O₂, N₂, CH₄ and CO₂ at 35°C over a range of pressures up to 20 atm. Sorption experiments were also done for N₂, CH₄, and CO₂ under the same conditions. The permeability coefficients of these polymers rank in the order:



for all of the gases. This order correlates well with free volume as well as with the γ transition temperature. The symmetric methyl substitution of TMPSF yields a relatively open structure with improved separation characteristics over PSF. The asymmetric substitution results in tightly packed structures for the dimethyl materials that are highly selective but less permeable than PSF or TMPSF. The flexible cyclohexyl substituent of DMPSF-Z further reduces the gas permeability and improves the selectivity.

(Keywords: polysulphones; permeation; sorption; diffusion; membranes)

INTRODUCTION

New materials with higher permeability and permselectivity than those currently available are required to continue to advance the technology of gas separations by membranes in present uses¹⁻⁸ and to open additional applications^{9,10}. Typically, a trade-off exists between permeability and selectivity among polymers that might be used as membranes. Nevertheless, a few examples that run counter to this general rule have been reported^{11,12}. Recent studies have been aimed at systematically varying polymer intrasegmental mobility and chain packing efficiency in order simultaneously to improve permeability and selectivity¹³⁻¹⁷. Such an approach necessitates a thorough understanding of the structural features that affect chain mobility and packing and the resultant effects on gas transport.

The present work is part of a study of a family of polysulphones in which systematic structural modifications have been made. The effect of these changes on gas transport properties is related to segmental mobility using thermal techniques and to chain packing by free-volume analysis. Further study of the polysulphones seems especially warranted because of the importance of bisphenol A polysulphone (PSF) in the field of membranes for gas separation. Asymmetric PSF hollow fibres were the first large-scale commercially accepted gas

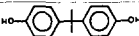
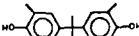
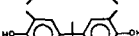

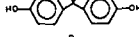
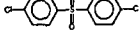
separation membrane system¹⁸ and continue to be widely used. Other composite membrane structures often include PSF as a porous support layer¹⁹. PSF has been chosen for membrane applications because of its processibility, chemical resistance, toughness and high T_g , in addition to its gas transport properties.

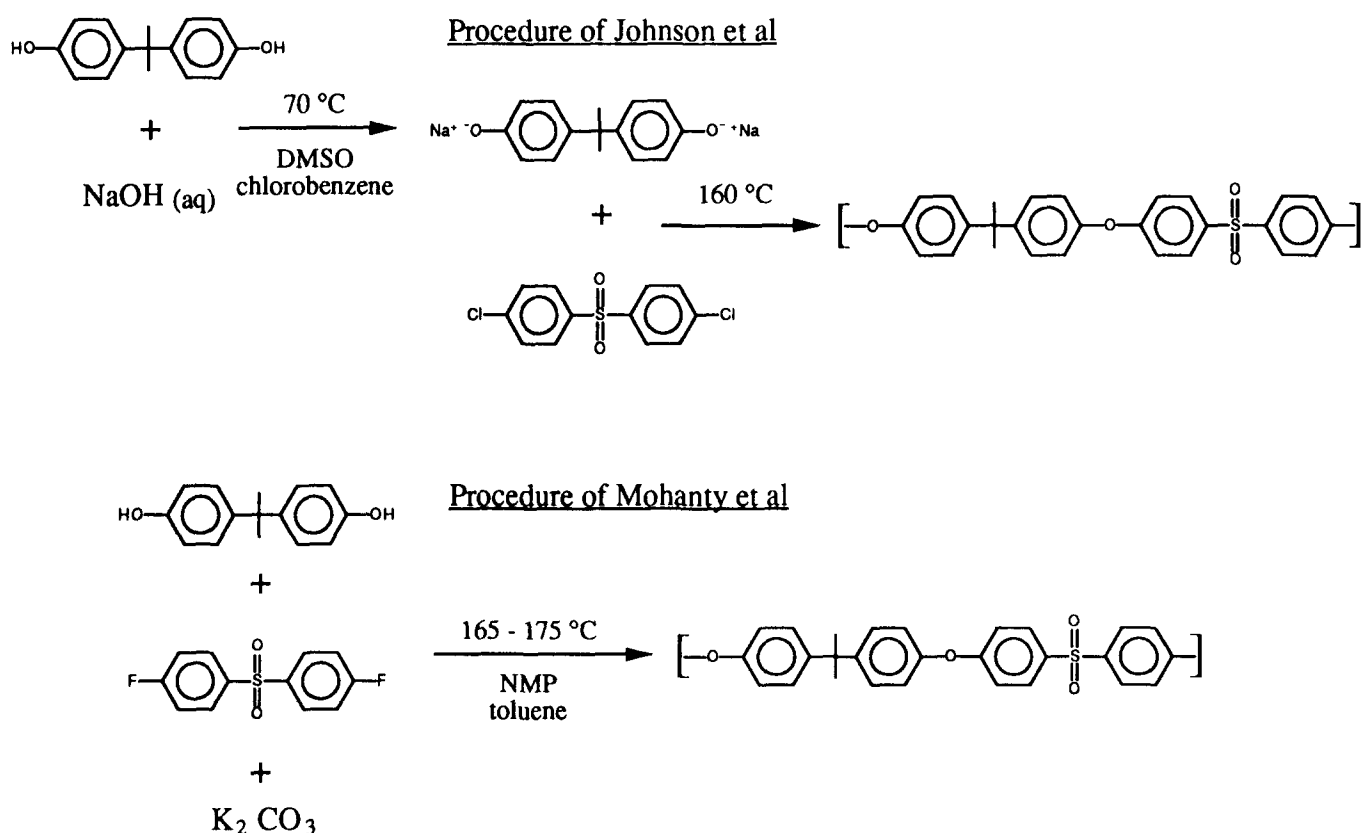
This paper deals with a set of polysulphones in which certain phenylene hydrogens are replaced by methyl groups. The analysis focuses on the differences between symmetric and asymmetric methyl substitution. The unsubstituted PSF is compared to symmetrically substituted tetramethyl bisphenol A polysulphone (TMPSF) and two asymmetrically substituted materials, dimethyl bisphenol A polysulphone (DMPSF) and dimethyl bisphenol Z polysulphone (DMPSF-Z). The effect of replacing the isopropylidene of DMPSF with a cyclohexyl group is also seen with DMPSF-Z. Structures for each of the polymers are presented in *Table 1* along with monomer and synthesis information. Prior gas sorption and transport measurements on PSF²⁰⁻²² and TMPSF²³ have been made in this laboratory. Results obtained here generally agree with those data. However, the TMPSF data of Pilato *et al.*¹¹, cited above, are somewhat inconsistent with these findings.

Two subsequent papers deal with the effect of replacing the isopropylidene unit of PSF and TMPSF with other molecular groups. A fourth paper will bring together a large amount of information obtained from the dynamic mechanical thermal testing of these and other polysulphones synthesized in this laboratory. This study will

* To whom correspondence should be addressed

Table 1 Monomer and synthesis information for polysulphones

Monomers			Synthesis			
Structure	Source	Recrystallization	Polymer	Method	Time (h)	$[\eta]$ (dl g ⁻¹) ^a
	Aldrich Chemical Co.	Toluene	PSF	Johnson <i>et al.</i> ²⁴	4	0.40
	Mitsubishi Gas Chemical Co.	Sublimed	TMPSF	Mohanty <i>et al.</i> ²⁵⁻²⁷	16	1.06
	Aldrich Chemical Co.	Toluene	DMPSF	Johnson <i>et al.</i> ²⁴	6	0.99
	Mitsui Petrochemical Ind.	None	DMPSF-Z	Mohanty <i>et al.</i> ²⁵⁻²⁷	16	1.12
	Aldrich Chemical Co.	Ethanol				
	Aldrich Chemical Co.	Sublimed				

^aIn chloroform at 25°C**Figure 1** Synthetic pathways used to make polysulphones²⁴⁻²⁷

focus on the details of the low-temperature γ transition and its relation to small-scale molecular motions.

MATERIALS AND PROCEDURES

Polymer synthesis

High-molecular-weight polysulphones were synthesized by the condensation of the appropriate bisphenol and a dihalogenated diphenylsulfone in the presence of a base. One of two procedures, described by Johnson *et al.*²⁴ and by Mohanty *et al.*²⁵⁻²⁷, was used for the polymerization. The reaction schemes for each procedure are shown in *Figure 1* for the formation of bisphenol A polysulphone. High-purity monomers were obtained from commercial sources and further purified by sublima-

tion or recrystallization from appropriate solvents (see *Table 1*).

Using the method of Johnson *et al.*, the bisphenol monomer is first reacted with aqueous sodium hydroxide at about 70°C in dimethylsulphoxide (DMSO) and chlorobenzene to form the disodium salt of the bisphenol. Water is removed from the system by azeotropic distillation with chlorobenzene. The temperature is then raised to 160°C, and 4,4'-dichlorodiphenylsulfone is added. After several hours of polymerization, the mixture is diluted with chlorobenzene and filtered to remove sodium chloride. The product polymer is then coagulated in ethanol and dried in a vacuum oven.

A few slight modifications to this procedure were made for convenience. First, the reactions were carried out in

a 500 ml glass resin kettle with a batch size of 0.10 mol. A well insulated Vigreux column equipped with a condenser was used for the fractionation and removal of the azeotropic distillate. The sulphone monomer was added in solid form rather than in solution. The reaction times used here were several times longer than those reported by Johnson *et al.*²⁴.

The method of Mohanty *et al.* uses potassium carbonate as the base rather than sodium hydroxide. Because potassium carbonate is a weaker base than sodium hydroxide, excess base can be added without fear of undesirable side reactions²⁸. Excess sodium hydroxide can react with the sulphone monomer, upsetting the polymerization stoichiometry, or can participate in chain cleavage reactions. Either case leads to a low-molecular-weight product. These problems are alleviated with the use of potassium carbonate.

The Mohanty procedure is also somewhat simpler experimentally. All of the reactants, which include the bisphenol, 4,4'-difluorodiphenylsulphone and potassium carbonate, are combined in 1-methyl-2-pyrrolidinone (NMP) and toluene. Here the fluorinated sulphone is used because of its greater reactivity than the chlorinated sulphone used above. The solution is gradually heated while water is removed by azeotropic distillation with toluene. After complete removal of water, polymerization is carried out at 165–175°C. The reaction mass is then diluted with toluene and filtered. The polymer is coagulated in ethanol and dried in a vacuum oven. In order completely to remove residual NMP, the polymer is redissolved in methylene chloride and coagulated in ethanol several times and finally dried above the glass transition temperature. In some cases, it was necessary to extract the NMP further in a Soxhlet apparatus²⁹ for several days before drying. Water and ethanol were used as extraction solvents.

Film preparation

Amorphous films 1–5 mil (0.025–0.125 mm) thick were prepared from each of the polymers by casting a 5–10 wt% solution in methylene chloride on a clean glass plate. The casting procedure was carried out in a glove bag to control the rate of solvent removal and to limit exposure to atmospheric water. After drying overnight in the glove bag, the films were removed from the glass plates and placed in a vacuum oven. The temperature was then gradually raised over several days to 10°C above the glass transition temperature of the polymer. After drying for two more days, the films were removed from the oven and cooled to room temperature over several minutes.

In order to evaluate the consistency of this film preparation technique, some preliminary experiments were undertaken. The gas permeability of several PSF films were tested and compared to data from previous studies^{20–22}. There was some variation according to researcher, and, in all cases, melt-extruded films were less permeable than solution-cast films. However, data for films prepared by the method discussed above were in excellent agreement with one another. The results from these experiments are given in the Appendix.

Gas sorption and transport

Pure gas permeability measurements were made for each of six gases using the standard permeation tech-

niques employed in this laboratory^{30,31}. Helium, hydrogen, oxygen, nitrogen, methane and carbon dioxide were tested at 35°C and in that order. For safety reasons, the maximum pressure used was limited for hydrogen and oxygen to 2 and 5 atm, respectively. Data were taken to 20 atm for the other four gases. In order to avoid the time-dependent hysteretic effects that can be caused by exposure to high-pressure gases, especially carbon dioxide³⁰, the permeability measurements were taken by stepping up from 1 atm with no prior exposure to high-pressure gas.

Pure gas sorption measurements were also made for nitrogen, methane and carbon dioxide from 1 to 20 atm at 35°C. Again, the data were taken in this order with no previous exposure to high-pressure carbon dioxide. The measurements were carried out using a pressure decay sorption cell as described elsewhere^{31–33}.

Characterization

The glass transition temperature for each polymer was determined by differential scanning calorimetry (d.s.c.) with a Perkin-Elmer DSC-7 at a scanning rate of 20°C min⁻¹. The samples were scanned twice consecutively as a means to check for solvent and annealing effects. The glass transition temperature T_g was taken as the midpoint of the heat capacity step change on the second scan. The more subtle secondary relaxation processes were examined by dynamic mechanical thermal analysis (d.m.t.a.) using the Imass Autovibron Dynamic Mechanical Viscoelastometer. The instrument was operated in the tensile mode at 110 Hz and at a heating rate of 1°C min⁻¹.

Dilute solution viscometry was used as a measure of the relative molecular weights of the polymers. The intrinsic viscosity for each polymer was obtained in chloroform at 25°C using a size 25 Cannon-Fenske viscometer.

Wide-angle X-ray diffraction (WAXD) measurements were performed on a Phillips X-ray diffractometer with Cu K α radiation having a wavelength of 1.54 Å. Because of the short-range order exhibited by amorphous polymers, a maximum is observed in the diffraction patterns of these polymers representative of their most probable intersegmental spacing³⁴. This intersegmental spacing, or d -spacing, can be calculated from the Bragg equation³⁵, $n\lambda = 2d \sin \theta$, at the angle of maximum reflective intensity.

The densities of the polymers were measured by flotation of small samples of film in a density gradient column maintained at 30°C. The column employs a degassed solution of aqueous calcium nitrate of varying concentration to provide the gradient. Glass beads of known density are used for calibration.

Free-volume calculation

The free volume of each of the polymers was obtained by subtracting a calculated occupied volume, V_0 , from the measured specific volume, V . The specific free volume (SFV) and fractional free volume (FFV) are given by:

$$SFV = V - V_0 \quad \text{or} \quad FFV = (V - V_0)/V \quad (1)$$

The group contribution methods of Bondi^{36,37} and of Sugden³⁸ can be used to calculate V_0 , which is an estimate of the molecular volume of the polymer at 0 K. In a previous paper dealing with structurally modified poly-

carbonates³⁹, the best statistical correlation between free volume and gas permeation and diffusion was found using the volume-based *FFV* computed by the Bondi method.

DYNAMIC MECHANICAL ANALYSIS

Background

A variety of techniques, including dielectric relaxation, nuclear magnetic resonance (n.m.r.) spectroscopy and dynamic mechanical thermal analysis (d.m.t.a.), have been used to probe the molecular motions in polyarylene ethers and related materials. These polymers exhibit several transition regions in the glassy state, which presumably can be associated with specific molecular phenomena. The transitions are generally labelled with the symbols α , β , γ , etc., in order from high to low temperature. Much of the work has been done on bisphenol A based polycarbonate (PC) and polysulphone (PSF). In d.m.t.a. experiments at a frequency of 110 Hz, transitions appear at about 160, 85 and -75°C for PC and at approximately 193, 85 and -80°C for PSF. The α transition corresponds to the onset of large-scale molecular motions associated with the glass-rubber transition⁴⁰. The small, broad β transition has been ascribed to either non-equilibrium packing defects created by quenching the sample from above the glass transition temperature⁴¹, or to orientational stresses introduced during processing⁴²⁻⁴⁴. This transition can be reduced or eliminated by annealing⁴¹⁻⁴⁴. Clearly, the β transition is highly dependent on sample preparation and thermal history. The γ transition in these materials is the result of small-scale molecular motions about flexible linkages in the polymer chain^{40,45}. It is this scale of mobility that may be related to the gas transport process. The broad γ transition is most likely a composite of several superimposed peaks associated with the different molecular groups that make up the repeat unit⁴⁵⁻⁴⁷. However, the exact nature of the molecular motions and the degree to which intramolecular and intermolecular factors play a role are still undetermined.

Results

The $\tan \delta$ curves from the dynamic mechanical spectra of each of the polysulphones are given in Figure 2. The curves are offset vertically with a shift of one order of magnitude between each one. The peaks are labelled as β or γ transitions. As mentioned above, β transitions are distinguished by their sensitivity to thermal treatment. The γ peaks arise because of small-scale motions of individual groups that make up the polymer repeat unit. For polymers that are largely aromatic, like these polysulphones, phenylene ring motions tend to be the most significant contributors to the γ transitions^{40,45,47}.

Substitution of phenylene hydrogens with methyl groups hinders these motions considerably. Two γ transitions appear for the substituted polysulphones. The γ_1 peak is ascribed to the motions of the substituted rings, while the γ_2 peak is associated with the unsubstituted rings. Neighbouring groups may also participate in these motions, as they seem to be somewhat cooperative^{40,46-48}. The γ_1 transition occurs at a higher temperature than the γ_2 transition due to greater steric hindrance and moment of inertia for the methyl-substituted rings than for their unsubstituted counter-

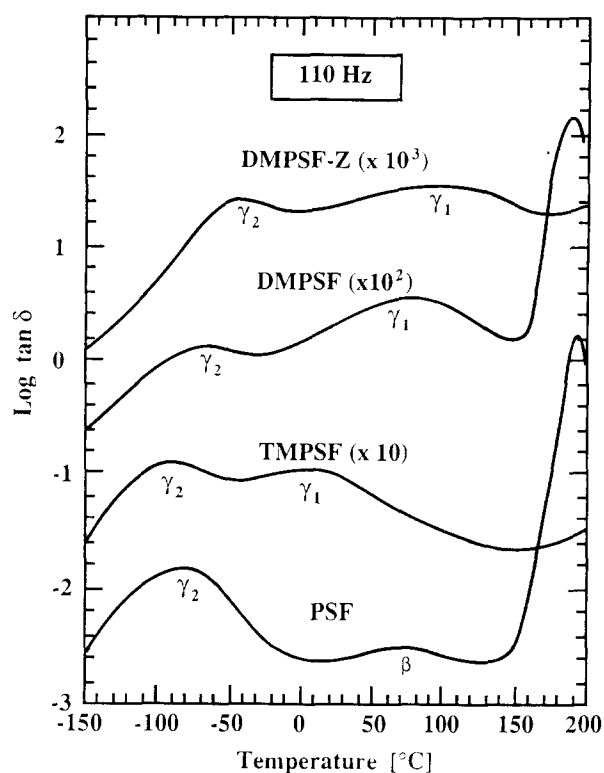


Figure 2 Loss tangent as a function of temperature from dynamic mechanical thermal analysis showing β and γ transitions

parts. Since all of the rings in PSF are unsubstituted, only one γ transition has been identified for this polymer. PSF does, however, exhibit a small β transition, which is not seen for the other materials. For the substituted polysulphones, this transition may be hidden by the larger γ_1 peak in the same temperature region. The magnitude of the γ_2 peak is sensitive to sorbed water^{45,49}, which suggests that the polar sulphone group also plays a major role in this transition.

Both intramolecular and intermolecular considerations determine the secondary relaxation behaviour of these materials. Because the units involved in the γ_2 transition are common to all of the polysulphones, this transition should be a good indicator of intermolecular effects. The temperature of the peak maximum is inversely related to free volume. Presumably, as the free volume is increased, intermolecular barriers to small-scale motions are reduced and the transition occurs at a lower temperature. There still may be some coupling of the γ motions between the substituted and unsubstituted portions of the repeat unit, which would restrict the mobility of the unsubstituted rings. This intramolecular effect would tend to lessen the intermolecular free-volume effect for TMPSF. For DMPSF and DMPSF-Z both intramolecular and intermolecular effects hinder the small-scale mobility of the unsubstituted half of the repeat unit. The location of the γ_1 transition follows a similar relationship with free volume. Here, intramolecular effects are more important due to the different substituents on the groups involved in the motions.

GAS SORPTION AND TRANSPORT

Permeation

Pure gas permeability isotherms for the six gases, CO_2 , CH_4 , O_2 , N_2 , He and H_2 , are shown as a function of

upstream driving pressure in Figures 3–8. The permeability coefficients of the four polysulphones rank in the order:

$$\text{TMPSF} \gg \text{PSF} \gg \text{DMPSF} > \text{DMPSF-Z}$$

for all of the gases. Split axes have been used on each of the plots to accommodate the exceptionally high permeability values for TMPSF. The permeability coefficients for CO₂, CH₄ and N₂ generally decrease with increasing pressure, while little pressure dependence is seen for O₂, He and H₂. This is the normal trend for glassy polymers in the absence of strong plasticization effects³⁰.

The calculated free-volume values, given in Table 2, follow the observed permeability ranking. The variation

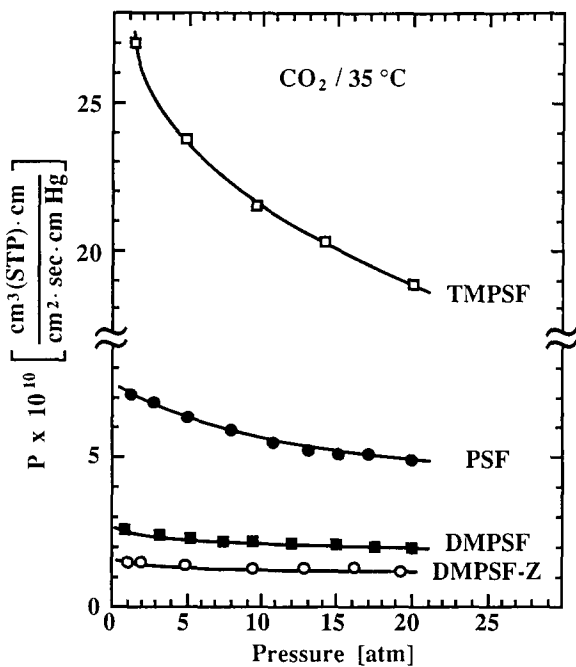


Figure 3 Pressure dependence of CO₂ permeability coefficient at 35°C

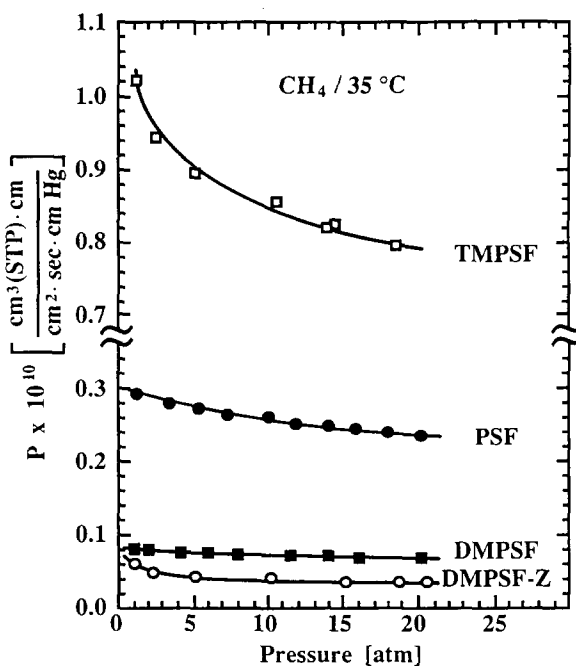


Figure 4 Pressure dependence of CH₄ permeability coefficient at 35°C

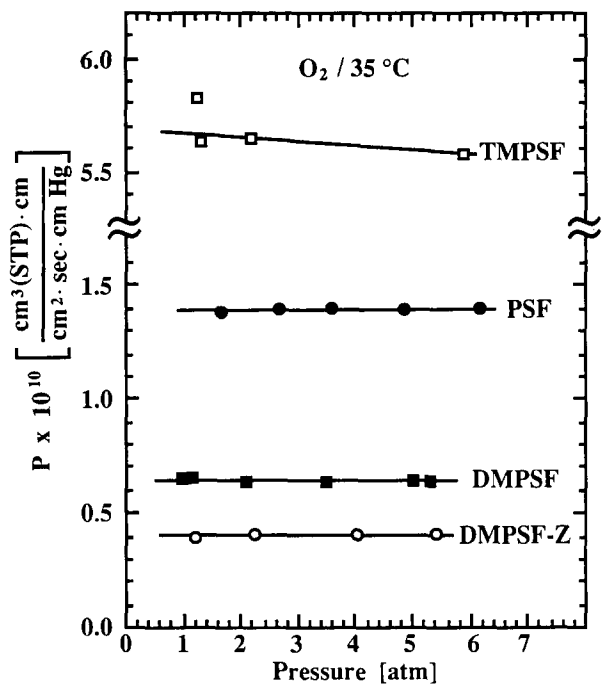


Figure 5 Pressure dependence of O₂ permeability coefficient at 35°C

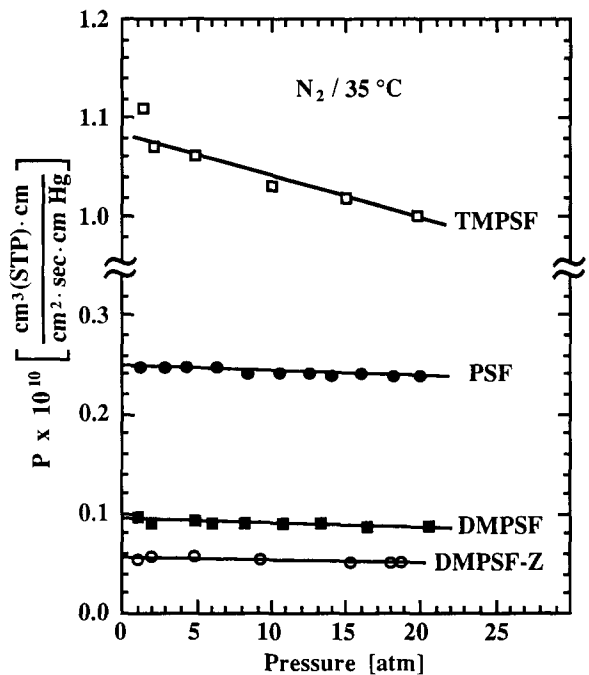


Figure 6 Pressure dependence of N₂ permeability coefficient at 35°C

of the X-ray diffraction *d*-spacing is also consistent with the free-volume and permeability data. TMPSF has the highest *FFV*, approximately 17.1% (calculated by the Bondi method), and the largest *d*-spacing of 5.5 Å. DMPSF and DMPSF-Z have lower values of *FFV*, 14.9% and 13.6%, respectively, with a *d*-spacing of 5.0 Å for each. The symmetric methyl substitution of TMPSF has resulted in a more open structure than PSF. According to the *d*-spacing, the TMPSF chains are approximately 10% further apart than those of PSF. The asymmetric methyl substitution of DMPSF and DMPSF-Z does not have this effect. The average chain spacing does not increase to accommodate the substituents. Instead, the methyl groups fill void space between

Table 2 Characterization of molecular packing for polysulphones

Polymer	ρ (g cm ⁻³)	<i>d</i> -spacing ^a (Å)	Bondi ^{36,37}		Sugden ³⁸	
			<i>SFV</i> ^b (cm ³ g ⁻¹)	<i>FFV</i> ^c	<i>SFV</i> (cm ³ g ⁻¹)	<i>FFV</i>
PSF	1.240	5.0	0.126	0.156	0.106	0.132
TMPSF	1.151	5.5	0.148	0.171	0.131	0.151
DMPSF	1.213	5.0	0.123	0.149	0.105	0.127
DMPSF-Z	1.227	5.0	0.111	0.136	0.091	0.111

^aX-ray diffraction, $\lambda = 1.54 \text{ \AA}$

^bSpecific free volume, $SFV = V - V_0$

^cFractional free volume, $FFV = (V - V_0)/V$

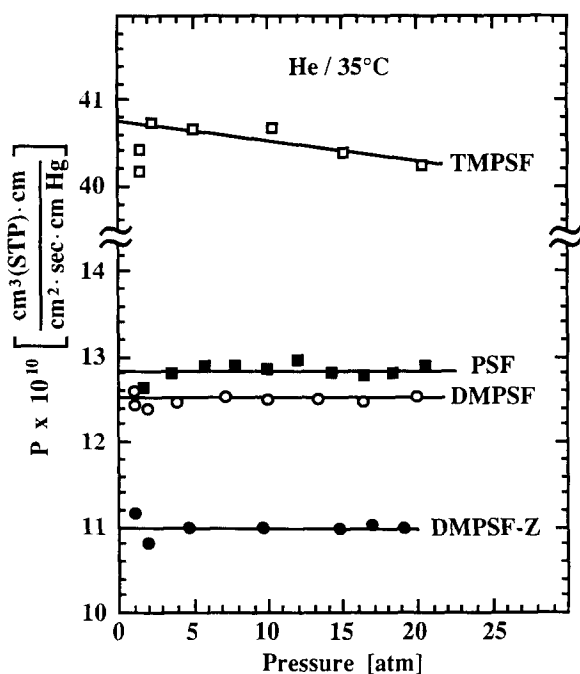


Figure 7 Pressure dependence of He permeability coefficient at 35°C

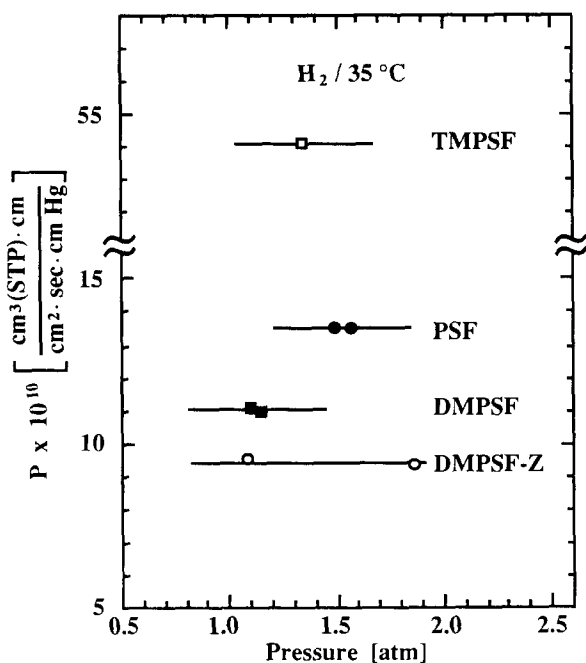


Figure 8 Pressure dependence of H₂ permeability coefficient at 35°C

Table 3 Thermal transitions for polysulphones

Polymer	D.s.c. ^a		D.m.t.a./110 Hz		
	<i>T_g</i> (°C)	<i>T_α</i> (°C)	<i>T_β</i> (°C)	<i>T_{γ1}</i> (°C)	<i>T_{γ2}</i> (°C)
PSF	186	193	85	–	–80
TMPSF	242	<i>b</i>	–	–10	–92
DMPSF	180	189	–	80	–60
DMPSF-Z	197	<i>b</i>	–	100	–35

^a20°C min⁻¹

^bOut of range (>200°C)

chains and result in less free volume. The cyclohexyl group of DMPSF-Z has the same effect and further reduces the free volume.

Thermal transition data, including d.s.c. and d.m.t.a. results, are given in Table 3. The d.s.c. data indicate that the symmetric methyl substitution results in a large chain-stiffening effect. The *T_g* of TMPSF, 242°C, is more than 50°C higher than that of PSF. One might expect DMPSF to be intermediate between PSF and TMPSF, but this is not the case. The asymmetric methyl substitution results in a *T_g* of 180°C for DMPSF, which is slightly lower than the 186°C glass transition temperature of PSF. The *T_g* of the dimethyl-substituted material is increased to 197°C when the isopropylidene unit is replaced with a cyclohexyl group. No direct correlation is apparent between these *T_g* values and the polymer gas transport properties.

On the other hand, the low-temperature γ transition does follow a trend, which can be related to gas transport behaviour. An inverse relationship exists between the γ peak temperatures and permeability. Presumably, this relationship arises because the more permeable materials have more free volume. As free volume increases, the intermolecular barriers to small-scale motions are reduced, and the associated transitions occur at lower temperatures.

The ideal separation factor, defined as the ratio of the pure component permeabilities:

$$\alpha_{AB}^* = P_A/P_B \quad (2)$$

provides a useful measure of the intrinsic permselectivity of a membrane material for mixtures of A and B for most cases³⁰. A comparison of the permeability coefficients and ideal separation factors for each of the polysulphones at a fixed pressure are shown in Table 4 for the following gas pairs, CO₂/CH₄, O₂/N₂, He/CH₄ and He/H₂. TMPSF is several times more permeable than PSF without any loss in selectivity. The dimethyl-substituted

Table 4 Permeability and selectivity for polysulphones at 35°C

Polymer	$P_{CO_2}^{a,d}$	α_{CO_2/CH_4}^* ^a	$P_{O_2}^{b,d}$	α_{O_2/N_2}^* ^b	$P_{He}^{a,d}$	α_{He/CH_4}^* ^a	α_{He/H_2}^* ^c
PSF	5.6	22	1.4	5.6	13	49	0.93
TMPSF	21	22	5.6	5.3	41	45	1.3
DMPSF	2.1	30	0.64	7.0	12	170	1.1
DMPSF-Z	1.4	34	0.41	7.2	11	280	1.2

^a10 atm

^b5 atm

^c1 atm

$$^d P \times 10^{10} \left(\frac{\text{cm}^3(\text{STP}) \text{ cm}}{\text{cm}^2 \text{ s cmHg}} \right)$$

materials, on the other hand, are less permeable than PSF, but have exceptionally high values for the ideal separation factor for each of the gas pairs. The selective nature of these materials is seen most dramatically for the He/CH₄ separation, which has the greatest size difference between penetrants. The He/CH₄ ideal separation factor of DMPSF-Z is more than five times that of PSF. Their O₂/N₂ separation factors, which are near 7 for both polymers, are also unusually high compared to most glassy polymers¹⁶.

Solubility and diffusivity contributions

Sorption isotherms for CO₂, CH₄ and N₂ are shown in Figures 9–11. The solubility coefficients generally rank in the order:

$$\text{TMPSF} > \text{PSF} > \text{DMPSF-Z} > \text{DMPSF}$$

The differences in gas solubility between these materials are much less pronounced than the differences in permeability.

For the case of negligible downstream pressure, the permeability coefficient can be written as:

$$P = \bar{D}\bar{S} \tag{3}$$

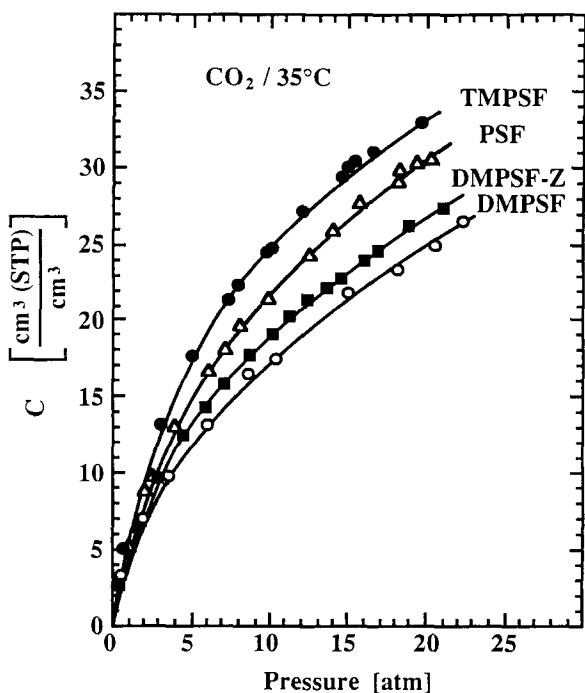


Figure 9 Sorption isotherms for CO₂ at 35°C

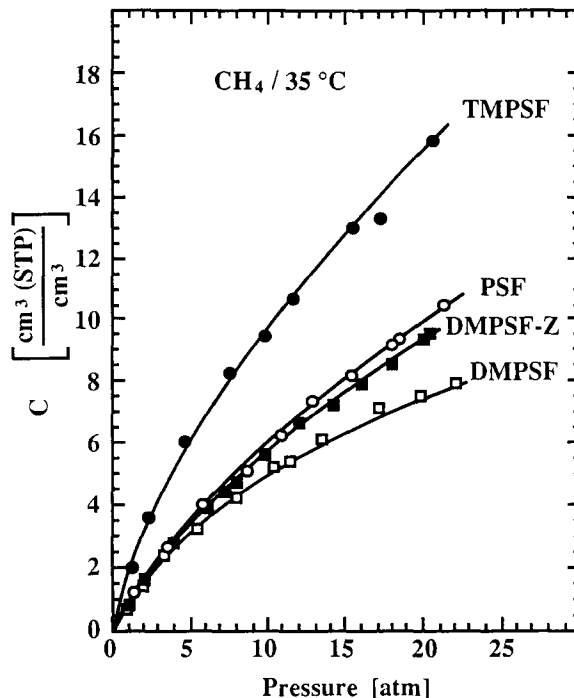


Figure 10 Sorption isotherms for CH₄ at 35°C

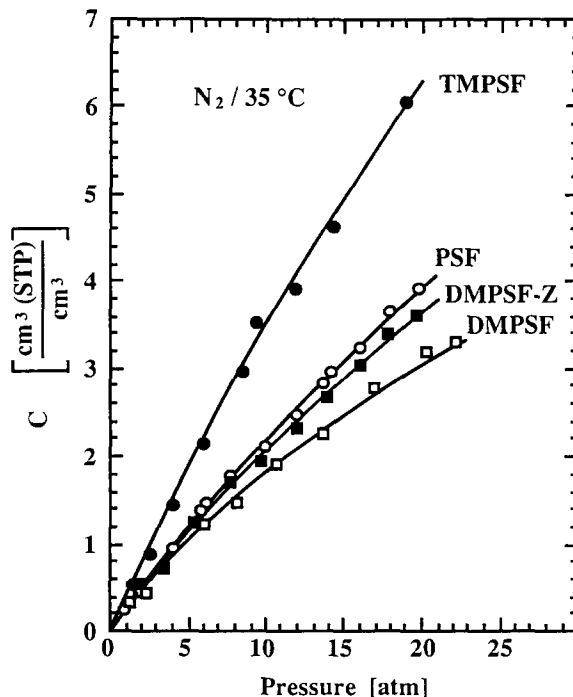


Figure 11 Sorption isotherms for N₂ at 35°C

Table 5 Solubility and diffusivity contributions to CO₂ and CH₄ permselectivity at 10 atm and 35°C

Polymer	$P_{\text{CO}_2}^a$	$\alpha_{\text{CO}_2/\text{CH}_4}^*$	$\bar{S}_{\text{CO}_2}^a$	$\bar{S}_{\text{CO}_2}/\bar{S}_{\text{CH}_4}$	$\bar{D}_{\text{CO}_2}^c$	$\bar{D}_{\text{CO}_2}/\bar{D}_{\text{CH}_4}$
PSF	5.6	22	2.1	3.7	2.0	5.9
TMPSF	21	22	2.5	2.7	6.4	8.1
DMPSF	2.1	30	1.7	3.3	0.94	9.1
DMPSF-Z	1.4	34	1.9	3.3	0.56	10

$$^a P \times 10^{10} \left(\frac{\text{cm}^3(\text{STP}) \text{ cm}}{\text{cm}^2 \text{ s cmHg}} \right)$$

$$^b S \left(\frac{\text{cm}^3(\text{STP})}{\text{cm}^3 \text{ atm}} \right)$$

$$^c D \times 10^8 \left(\frac{\text{cm}^2}{\text{s}} \right)$$

Table 6 Solubility and diffusivity contributions to O₂ and N₂ permselectivity at 5 atm and 35°C

Polymer	$P_{\text{O}_2}^a$	$\alpha_{\text{O}_2/\text{N}_2}^*$	$S_{\text{appO}_2}^b$	$S_{\text{O}_2}/S_{\text{N}_2}$	$D_{\text{appO}_2}^{c,d}$	$D_{\text{O}_2}/D_{\text{N}_2}$
PSF	1.4	5.6	0.24	1.6	4.4	3.6
TMPSF	5.6	5.3	0.53	1.4	8.0	3.8
DMPSF	0.64	7.0	0.29	1.7	1.7	4.2
DMPSF-Z	0.41	7.2	0.28	1.5	1.1	4.8

$$^a P \times 10^{10} \left(\frac{\text{cm}^3(\text{STP}) \text{ cm}}{\text{cm}^2 \text{ s cmHg}} \right)$$

$$^b S \left(\frac{\text{cm}^3(\text{STP})}{\text{cm}^3 \text{ atm}} \right)$$

$$^c D \times 10^8 \left(\frac{\text{cm}^2}{\text{s}} \right)$$

^d Estimated from permeation time lag

where \bar{D} is a diffusion coefficient averaged across the membrane thickness and \bar{S} is a solubility coefficient obtained from the secant slope of the sorption isotherm at the upstream conditions⁵⁰. The diffusion coefficient can then be calculated from independent permeation and solubility experiments. For cases where solubility data are unavailable, an apparent diffusion coefficient can be estimated from the membrane thickness l and the time lag θ from a transient permeation measurement^{30,31}:

$$D_{\text{app}} = l^2 / (6\theta) \quad (4)$$

The solubility and diffusivity contributions to the permselectivity of each polymer are given in *Tables 5* and *6* for the CO₂/CH₄ and O₂/N₂ separations. Both solubility and diffusivity effects play a role in the differences in permeability observed within this set of polysulphones. In general, however, the diffusive effects are larger. For example, the CO₂ solubility coefficient of TMPSF is only 20% larger than that of PSF, while the CO₂ diffusion coefficient of TMPSF is 3.2 times that of PSF. The variation in selectivity among these polymers is also primarily diffusion-controlled. The large mobility selectivity values for the methyl-substituted polysulphones result in relatively high separation factors. The gas mobility differences among the polymers tend to be more significant than the gas solubility differences, so the ideal separation factor follows the trend of the mobility selectivity.

Dual-mode analysis. According to the dual-mode sorption model^{51,52}, gas sorption in glassy polymers can be described as a function of pressure by:

$$C = k_D p + \frac{C_H b}{1 + b p} p \quad (5)$$

Table 7 Dual-mode sorption parameters for polysulphones at 35°C

Polymer	Gas	k_D $\left(\frac{\text{cm}^3(\text{STP})}{\text{cm}^3 \text{ atm}} \right)$	C_H $\left(\frac{\text{cm}^3(\text{STP})}{\text{cm}^3} \right)$	b (atm ⁻¹)
PSF	N ₂	0.166	0.957	0.104
	CH ₄	0.257	6.58	0.0901
	CO ₂	0.728	19.6	0.260
TMPSF	N ₂	0.225	3.74	0.0461
	CH ₄	0.460	7.26	0.233
	CO ₂	0.597	26.0	0.261
DMPSF	N ₂	Fit does not converge		
	CH ₄	0.135	8.64	0.0564
	CO ₂	0.505	17.8	0.235
DMPSF-Z	N ₂	0.153	0.694	0.196
	CH ₄	0.330	5.21	0.0907
	CO ₂	0.560	18.6	0.252

where the subscripts D and H represent Henry's law mode sorption and Langmuir mode sorption, respectively. The parameter k_D is the Henry's law solubility coefficient, C_H is the Langmuir sorption capacity and b is an affinity parameter characterizing the ratio of the rate constants for sorption and desorption. Fitting the sorption isotherms from *Figures 9–11* with the dual-mode model yields the parameters listed in *Table 7*. The statistical analysis was carried out using a SAS program with the Marquardt least-squares method⁵³.

The populations in each of the sorption modes can be assigned separate diffusion coefficients, D_D and D_H . Based on this dual-mobility model^{54,55}, for the case of negligible downstream pressure, the permeability coefficient can be

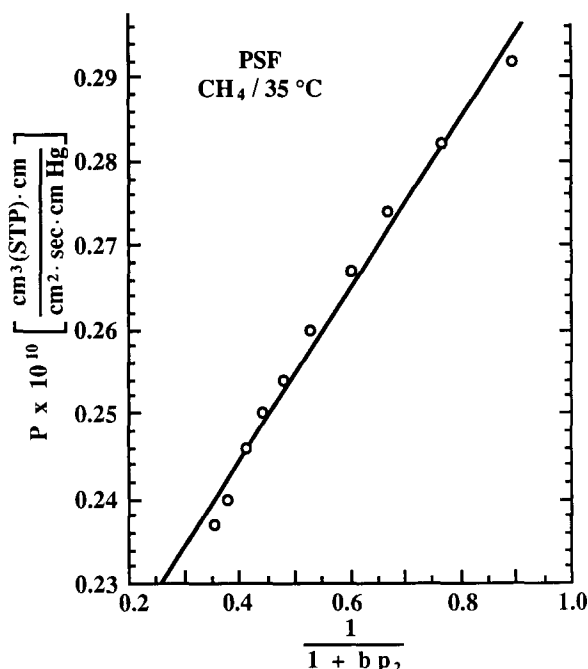


Figure 12 Correlation of CH₄ permeability coefficient at 35°C for PSF with dual-mode quantity $1/(1 + bp_2)$

Table 8 Dual-mode diffusion coefficients for polysulphones at 35°C

Polymer	Gas	$D_D \times 10^8$ ($\frac{\text{cm}^2}{\text{s}}$)	$D_H \times 10^8$ ($\frac{\text{cm}^2}{\text{s}}$)
PSF	N ₂	1.06	0.151
	CH ₄	0.602	0.131
	CO ₂	4.64	0.575
TMPSF	N ₂	2.57	1.57
	CH ₄	1.22	0.159
	CO ₂	22.0	1.54
DMPSF	CH ₄	0.312	0.0422
	CO ₂	2.80	0.179
DMPSF-Z	N ₂	0.246	0.0662
	CH ₄	0.0621	0.0393
	CO ₂	1.62	0.0770

written as:

$$P = k_D D_D \left(1 + \frac{FK}{1 + bp_2} \right) \quad (6)$$

with

$$K = C'_H b / k_D \quad \text{and} \quad F = D_H / D_D$$

The diffusion coefficients can then be readily calculated from the slope and intercept of an experimental plot of permeability *versus* $1/(1 + bp_2)$. An example of such a plot is shown in Figure 12 for CH₄ permeation in PSF. The diffusion coefficients obtained by this analysis are given in Table 8.

CONCLUSIONS

The replacement of phenylene hydrogens of polysulphone with methyl groups has been shown to have a significant effect on gas transport as well as other properties. The nature of these effects depends on the placement of the substituents. Symmetric methyl placement, as in TMPSF,

results in a high degree of chain stiffness, as judged by the effect on T_g , and a relatively open polymer matrix. The asymmetric substitution of DMPSF has the opposite effect, yielding a relatively low-free-volume structure with moderate chain stiffness. Replacement of the isopropylidene of DMPSF with a cyclohexyl group, as in DMPSF-Z, increases the T_g , but further reduces the free volume. The cyclohexyl group is bulky but flexible and can apparently change conformations to pack closely with other neighbouring molecular groups.

The relative gas transport rates of these materials agree well, at least qualitatively, with free-volume values calculated from group contribution methods³⁶⁻³⁸. The position of the low-temperature γ transition, indicative of small-scale molecular motions, also follows an identifiable trend with free volume and gas transport rate. Clearly, the same intramolecular and intermolecular factors that affect the gas transport characteristics of a polymer, i.e. chain stiffness and chain packing, are also major issues in determining its transition behaviour.

The combination of chain stiffness and high free volume makes TMPSF especially suited for gas separations. TMPSF is several times more permeable than PSF with similar selectivity. The dimethyl-substituted polymers, on the other hand, are less permeable than PSF, but their more closed structures lead to very high selectivity. Their O₂/N₂ separation factors, both near 7, are exceptionally high. Because the methyl and cyclohexyl substituents are simple hydrocarbon groups on a primarily hydrocarbon backbone, their major effect is on such structural factors as chain geometry, flexibility and packing rather than on molecular interactions. For this reason, the differences in gas transport properties are, for the most part, diffusion-controlled. The diffusion coefficient for a particular gas is much more sensitive to physical changes like polymer free volume and chain mobility than is the solubility coefficient.

The gas transport properties of TMPSF, when compared to PSF, show that the usual trade-off between permeability and selectivity may not always be strictly followed. Bulky and immobile substituents that simultaneously increase chain stiffness and decrease packing efficiency can result in improved separation characteristics. Asymmetric phenylene ring substitutions or placement of large, flexible groups in the backbone do not have this effect but still may be useful in making highly selective materials.

ACKNOWLEDGEMENTS

This research has been supported by the Department of Energy, Basic Sciences Program, through grant DE-FG05-86ER13507 and the Separations Research Program at The University of Texas at Austin. Acknowledgement is also made to the National Science Foundation and the Phillips Petroleum Foundation for fellowship support to J. S. McHattie.

REFERENCES

- Gardner, R. J., Crane, R. A. and Hannan, J. F. *Chem. Eng. Prog.* 1977, **73**, 76
- Bollinger, W. A., MacLean, D. L. and Narayan, R. S. *Chem. Eng. Prog.* 1982, **78**, 27
- Schell, W. J. and Houston, D. D. *Chem. Eng. Prog.* 1982, **78**, 33; *Hydrocarb. Process.* 1982, **61** (9), 249
- Lane, V. O. *Hydrocarb. Process.* 1983, **62** (8), 56

5 Mazur, W. H. and Chan, M. C. *Chem. Eng. Prog.* 1982, **78**, 38
 6 Coady, A. B. and Davis, J. A. *Chem. Eng. Prog.* 1982, **78**, 45
 7 Schendel, R. L., Mariz, C. L. and Mak, J. Y. *Hydrocarb. Process.* 1983, **62** (8), 58
 8 Parkinson, G. *Chem. Eng.* 1984, **91** (8), 14
 9 Spillman, R. W. *Chem. Eng. Prog.* 1989, **85**, 41
 10 Weber, W. F. and Bowman, W. *Chem. Eng. Prog.* 1986, **82**, 23
 11 Pilato, L., Litz, L., Hargitay, B., Osborne, R. C., Farnham, A., Kawakami, J., Fritze, P. and McGrath, J. E. *Polym. Prepr., Am. Chem. Soc., Div. Polym. Chem.* 1975, **16**, 42
 12 Pye, D. G., Hoehn, H. H. and Panar, M. J. *J. Appl. Polym. Sci.* 1976, **20**, 287
 13 Kim, T. H., Koros, W. J., Husk, G. R. and O'Brien, K. C. *J. Membr. Sci.* 1982, **37**, 45
 14 Kim, T. H., Koros, W. J. and Husk, G. R. *Sep. Sci. Tech.* 1988, **23**, 1611
 15 Muruganandam, N., Koros, W. J. and Paul, D. R. *J. Polym. Sci., Polym. Phys. Edn.* 1987, **25**, 1999
 16 Muruganandam, N. and Paul, D. R. *J. Membr. Sci.* 1987, **34**, 185
 17 Hellums, M. W., Koros, W. J., Husk, G. R. and Paul, D. R. *J. Membr. Sci.* 1989, **46**, 93
 18 Henis, J. M. S. and Tripodi, M. K. *Sep. Sci. Tech.* 1980, **15**, 1059
 19 Lundy, K. A. and Cabasso, I. *Ind. Eng. Chem. Res.* 1989, **28**, 742
 20 Barbari, T. A., Koros, W. J. and Paul, D. R. *J. Polym. Sci., Polym. Phys. Edn.* 1988, **26**, 709
 21 Maeda, Y. and Paul, D. R. *J. Polym. Sci., Polym. Phys. Edn.* 1987, **25**, 957
 22 Erb, A. J. and Paul, D. R. *J. Membr. Sci.* 1981, **8**, 11
 23 Moe, M. B., Koros, W. J. and Paul, D. R. *J. Polym. Sci., Polym. Phys. Edn.* 1988, **26**, 1
 24 Johnson, R. N., Farnham, A. G., Clendinning, R. A., Hale, W. F. and Merriam, C. N. *J. Polym. Sci. (A-1)* 1967, **5**, 2375
 25 Mohanty, D. K., Hedrick, J. L., Gobetz, K., Johnson, B. C., Yilgor, I., Yilgor, E., Yang, R. and McGrath, J. E. *Polym. Prepr., Am. Chem. Soc., Div. Polym. Chem.* 1982, **23** (1), 284
 26 Mohanty, D. K., Sachdeva, Y., Hedrick, J. L., Wolfe, J. F. and McGrath, J. E. *Polym. Prepr., Am. Chem. Soc., Div. Polym. Chem.* 1984, **25** (2), 19
 27 Mohanty, D. K. PhD Dissertation, Virginia Polytechnic Institute, 1983
 28 Mohanty, D. K. and McGrath, J. E. *Polym. Sci. Tech., Adv. Polym. Symp.* 1985, **31**, 113
 29 Mohanty, D. K., Wu, S. D. and McGrath, J. E. *Polym. Prepr., Am. Chem. Soc., Div. Polym. Chem.* 1988, **29** (1), 352
 30 O'Brien, K. C., Koros, W. J., Barbari, T. A. and Sanders, E. S. *J. Membr. Sci.* 1986, **29**, 229
 31 Koros, W. J., Chan, A. H. and Paul, D. R. *J. Membr. Sci.* 1977, **2**, 165
 32 Koros, W. J. and Paul, D. R. *J. Polym. Sci., Polym. Phys. Edn.* 1976, **14**, 1903
 33 Koros, W. J. PhD Dissertation, The University of Texas at Austin, 1977
 34 Alexander, L. E. 'X-Ray Diffraction in Polymer Science', Wiley, New York, 1969
 35 Schwartz, L. H. and Cohen, J. B. 'Diffraction from Materials', Academic Press, New York, Ch. 3
 36 Bondi, A. *J. Phys. Chem.* 1964, **44**, 1
 37 Bondi, A. 'Physical Properties of Molecular Crystals, Liquids, and Glasses', Wiley, New York, 1968
 38 Sugden, S. *J. Chem. Soc.* 1927, 1786
 39 McHattie, J. S., Koros, W. J. and Paul, D. R. *J. Polym. Sci., Polym. Phys. Edn.* 1989, **??**, **????**
 40 Yee, A. F. and Smith, S. A. *Macromolecules* 1980, **14** (1), 54
 41 Goldstein, M. 'Amorphous Materials', Wiley-Interscience, London, 1972
 42 Illers, K. H. and Breuer, H. *J. Colloid Sci.* 1963, **18**, 1
 43 LeGrand, D. G. *J. Appl. Polym. Sci.* 1969, **13**, 2129
 44 LeGrand, D. G. and Erhardt, P. F. *J. Appl. Polym. Sci.* 1969, **13**, 1707
 45 Robeson, L. M., Farnham, A. G. and McGrath, J. E. *Midl. Macromol. Monogr.* 1978, **4**, 405
 46 Vardarajan, K. and Boyer, R. F. *J. Polym. Sci., Polym. Phys. Edn.* 1982, **20**, 141
 47 Chung, C. I. and Sauer, J. A. *J. Polym. Sci. (A-2)* 1971, **9**, 1097
 48 Ratto, J. A., Inglefield, P. T., Rutowski, R. A., Li, K. L., Jones, A. A. and Roy, A. K. *J. Polym. Sci., Polym. Phys. Edn.* 1987, **25**, 1419
 49 Allen, G., McAinsh, J. and Jeffs, G. M. *Polymer* 1971, **12**, 85
 50 Chern, R. T., Koros, W. J., Hopfenberg, H. B. and Stannett, V. T. *J. Polym. Sci., Polym. Phys. Edn.* 1984, **22**, 1061

51 Barrer, R. M., Barrie, J. A. and Slater, J. *J. Polym. Sci.* 1958, **27**, 177
 52 Vieth, W. R., Howell, J. M. and Hsieh, J. H. *J. Membr. Sci.* 1976, **1**, 177
 53 Marquardt, D. W. *J. Soc. Ind. Appl. Math.* 1963, **2**, 431
 54 Koros, W. J. and Paul, D. R. *J. Polym. Sci., Polym. Phys. Edn.* 1978, **16**, 1947
 55 Petropoulos, J. H. *J. Polym. Sci.* 1970, **8**, 1797

APPENDIX

The gas sorption and transport properties of bisphenol A polysulphone (PSF) have been characterized previously by several researchers in this laboratory²⁰⁻²². The PSF samples for these studies were melt-extruded sheets of Udel P1700 supplied by the Union Carbide Corp. Films were tested as-received or solution-cast from methylene chloride. The CO₂ and CH₄ permeability isotherms from these studies are given as a function of upstream driving pressure at 35°C in Figures 13 and 14, respectively. The results vary somewhat depending on both the researcher and the processing history of the film. In all cases, however, the solution-cast films are more permeable than the melt-extruded ones.

In the present study, a number of polysulphones, including PSF, were synthesized in this laboratory. As a means to standardize the film preparation technique and to compare the experimental PSF with the commercial materials, gas permeation measurements were made on each of three new films. The first was the melt-extruded Udel P1700 film as-received, comparable to those

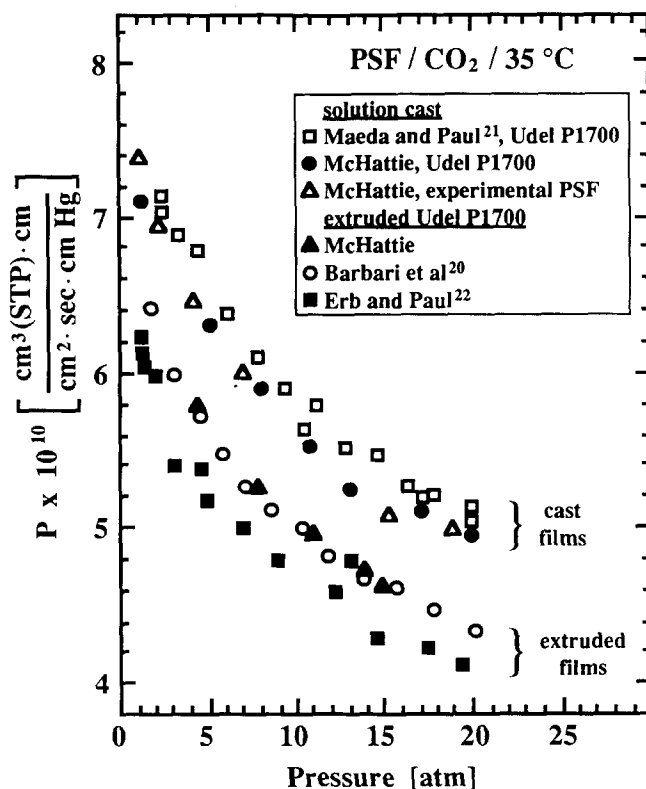


Figure 13 Comparison of the pressure dependence of the CO₂ permeability coefficient at 35°C for various solution-cast and extruded films of bisphenol A polysulphone

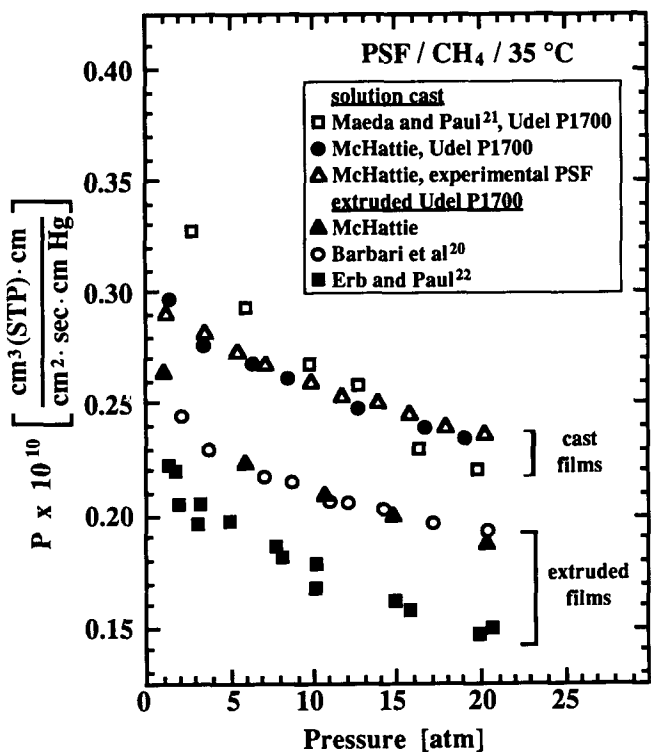


Figure 14 Comparison of the pressure dependence of the CH₄ permeability coefficient at 35°C for various solution-cast and extruded films of bisphenol A polysulphone

discussed above. The second was taken from the same Udel P1700 sheet, but was dissolved and solution-cast from methylene chloride. Finally, a third film was made from the experimental PSF by the same solution-casting procedure.

The CO₂ and CH₄ permeability isotherms for these three films are also given in Figures 13 and 14. Again, the solution-cast Udel P1700 is more permeable than the melt-extruded film. At 10 atm, the CO₂ permeability coefficient of the solution-cast film is about 12% greater than that of the melt-extruded sample. For CH₄ at 10 atm, this effect is about 24%. As a result, the CO₂/CH₄ permselectivity is also affected by the processing history. The CO₂/CH₄ separation factor at this pressure is 21.5 for the cast film and 23.8 for the extruded film. The solution-casting procedure yields films that are more permeable and less selective than melt-extruded films of the same material.

The data for the solution-cast films of the experimental PSF agree well with those of the solution-cast Udel P1700. This is an indication that the synthesis procedure yields a material that is similar to the commercial polymer. Also, the solution-casting method can be used as a consistent film preparation technique for comparing other polymers with different molecular structures.